THE SPS TARGET STATION FOR CHORUS AND NOMAD NEUTRINO EXPERIMENTS

S. Péraire, M. Ross and J.M. Zazula, CERN, Geneva, Switzerland

Abstract

A new SPS target station, T9, has been constructed for the CHORUS and NOMAD neutrino experiments at CERN. The heart of the station is the target box: 11 beryllium rods are aligned in a cast aluminium box; they are cooled by a closed circuit helium gas with adjusted flow to each rod. The box is motorised horizontally and vertically at both ends, to remotely optimise the secondary particle production by aligning the target with the incident proton beam. Radiation protection around the station is guaranteed by more than 100 tons of shielding material (iron, copper, marble). This presentation describes briefly the various components of the target station; it emphasises particularly the thermal and mechanical calculations which define a safe maximum beam intensity on the beryllium rods. Over the first two years of successful operation, the station has received more than $2{\cdot}10^{19}$ protons at 450 GeV/*c*, with intensity peaks of $2.8{\cdot}10^{13}$ protons per machine cycle.

1 GENERAL DESCRIPTION

The experience gained with the previous neutrino target station [1] directed the improvement effort in three main fields: alignment, cooling, shielding. The target box alignment is facilitated by 4 independent displacements. To improve cooling, the helium flow to each rod is adjusted according to the calculated energy deposition (see Section 2). A downstream collimator is incorporated in the shielding, which latter, being free of any mechanical function, is of simple and inexpensive construction.

1.1 Target box

The cast aluminium box contains 11 beryllium rods of ϕ 3 mm by 10 cm long, spaced every 9 cm. Each one is supported by two thin (2 mm) hollowed out beryllium disks, which ensure its lateral positional precision and a certain axial freedom. The two disks are fixed to a U-shaped aluminium support, and the supports are aligned by a channel milled in the bottom of the box. The alignment precision of the rods is $\pm$0.03 mm. Three longitudinal conduits, cast into the structure, ensure the circulation of the coolant; they are extended upstream by stainless steel tubes which traverse the shielding. The inlet conduits terminate with 22 stainless steel jets, disposed in opposing pairs either side of each rod. The box is sealed by a bolted aluminium cover, and by two titanium beam windows ϕ 60 mm by 0.1 mm thick. The horizontal and vertical displacement ($\pm$ 12 mm) of each end of the box is achieved by mechanisms driven by DC motors lodged in the shielding. These mechanisms have 3 support cups (2 upstream), upon which the box is precisely positioned. The transmission shafts, with universal couplings between motor and mechanism, traverse the shielding. A preliminary alignment was realised during installation, and refined successively to optimise beam efficiency [2].

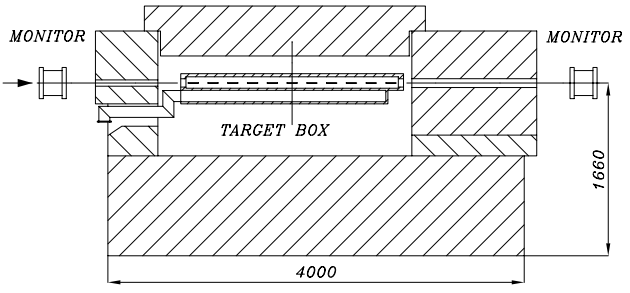

Figure 1: Layout of the new SPS T9 target station.

1.2 Helium cooling

Helium flow from each pair of jets was calibrated experimentally, by means of diaphragms of differing diameter positioned at their entries. Flow is maximal on the second rod (about 50 l/s), and diminishes progressively to the last one (about 10 l/s). The gas flow is provided by a 1465 turns/mn Roots pump delivering 2000 m^3/h at atmospheric pressure to the target box, via two water cooled heat exchangers and over 20 m of flexible piping. This circuit, fitted with numerous joints, is not perfectly leak tight (which would be unnecessary and expensive); consequently, the helium system is purged twice per week during periods of operation. The heat transfer coefficient between beryllium and helium (about 500 W/$m^2{\cdot}^o$C, for the first rod) was measured in a similar laboratory test installation, by replacing helium with air and beryllium with steel.

1.3 Shielding

The shielding encloses the target box and its mechanisms; it ensures a radiation dose compatible with restricted access areas. The shielding base supports 2 lateral walls (one mobile) and 2 collimators. The upstream collimator (ϕ 60 mm) is mobile; the downstream copper collimator (ϕ 85 mm) is of four parts, each cooled by an independent water circuit. The shielding assembly is surmounted by a mobile cover.

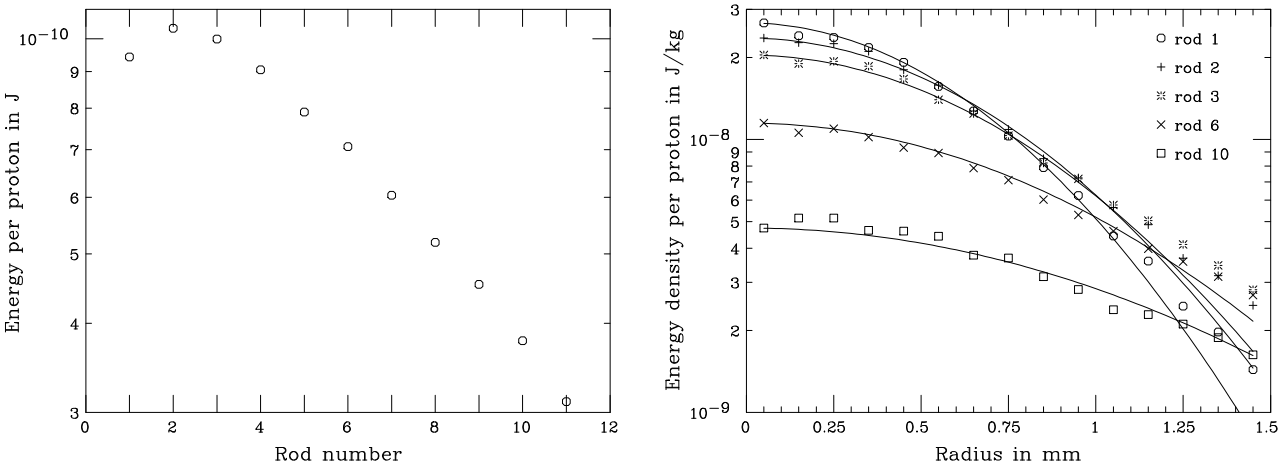

Figure 2: Spatial distribution of deposited energy: a) total energies absorbed by successive target rods (left plot); b) energy densities longitudinally averaged over rod length, as a function of radial distance off-axis (right plot).

The passage side is protected by additional 40 cm of marble. Most of the shielding elements (iron and marble) are constructed from recuperated and bolted material. Interior ventilation, initially provided, is no longer used. Handling of all the mobile elements (including the target box) is assured by an overhead mobile 7 ton crane, the manoeuvre being facilitated by leading marks on the rack and chariot. Maintenance and dismantling operations may be studied beforehand with the aid of a wooden model and video film.

2 ENERGY DEPOSITION, THERMAL AND STRESS ANALYSES

The maximum number of protons that can be put into the target is limited by the thermal and mechanical resistance of the rod material; thus the internal temperatures and stresses must be known with a sufficient precision. These cannot be measured in the operating conditions of the accelerator, view the small size of the target rods, extremely short extraction periods, and the surrounding high radiation level. Therefore theoretical predictions, based on the knowledge of beam parameters (energy, intensity, size and extraction duration), on the particle cascade and energy deposition simulations, and on the subsequent thermal and mechanical analyses, are of extreme interest. The deposited energy densities, estimated from primary and secondary simulations with the Monte Carlo (MC) shower code FLUKA [3] were converted to internal heat generation rates, taken as a thermal load input for the Finite-Element (FE) engineering analysis system ANSYS [4]; the transient solution results in space distributions and time evolution of the temperature and stress.

2.1 Simulations of particle cascades

For energy density study, it is sufficient to consider only the 11 beryllium target rods. They are axially irradiated by a 450 GeV/c mono-energetic proton beam, of identical horizontal and vertical Gaussian profiles (σ_h=σ_v=0.5 mm). The interactions, transport and energy deposition processes were followed down to the kinetic energy threshold of 0.1 MeV for all charged particles (hadrons, muons and electrons), down to 10 keV for photons, and down to 0.4 eV for neutrons. The energy density in each rod was scored using cylindrical-binning mesh with 10 longitudinal steps of Δz=1 cm and 15 radial steps of Δr=0.1 mm. Further details of the simulations can be found in our report [5].

Figure 2 shows total energies absorbed by successive beryllium rods (left plot), and energy density as a function of the radial distance off-axis (right plot). The results indicate the first rod as the most critical one: the deposited energy reaches the maximum density of 0.44 GeV/cm^3 per primary proton at about 8.5 cm depth in the beryllium; moreover, the longitudinal and radial gradient of energy deposition is steepest for the first 10 cm. Thus, maximum temperatures and resultant thermal stresses have to be expected in the first rod, even though the total energy absorbed by the second rod is slightly higher.

2.2 Transient thermo-mechanical analysis

Assuming an azimuthal symmetry of energy deposition, a rod could be modelled as a cylindrical unconstrained system (ends of rods having axial freedom of movement in support disks). The model was designed with the use of a 2-dimensional 4-node axisymmetric element (PLANE13, in the ANSYS library), of the coupled temperature and nodal displacement degrees of freedom, and with the internal heat generation load input. The model (longitudinal half-section through the rod) was meshed with 300 quadrilateral elements: 20 uniform divisions longitudinally, and 15 logarithmically increasing radial divisions. The constant and temperature-dependent beryllium properties are given in Ref. [5]. The cooling was accounted for by a surface convection boundary condition; the helium bulk temperature was assumed constant at 20^{o}C .

We assume that all the energy deposited in a rod by primaries and secondaries of a cascade is locally, immediately, and totally transformed into internal energy. An interface program linearly interpolates the energy density results from the MC scoring bins (read from the output file of FLUKA), to the subsequent node positions (read from the ANSYS

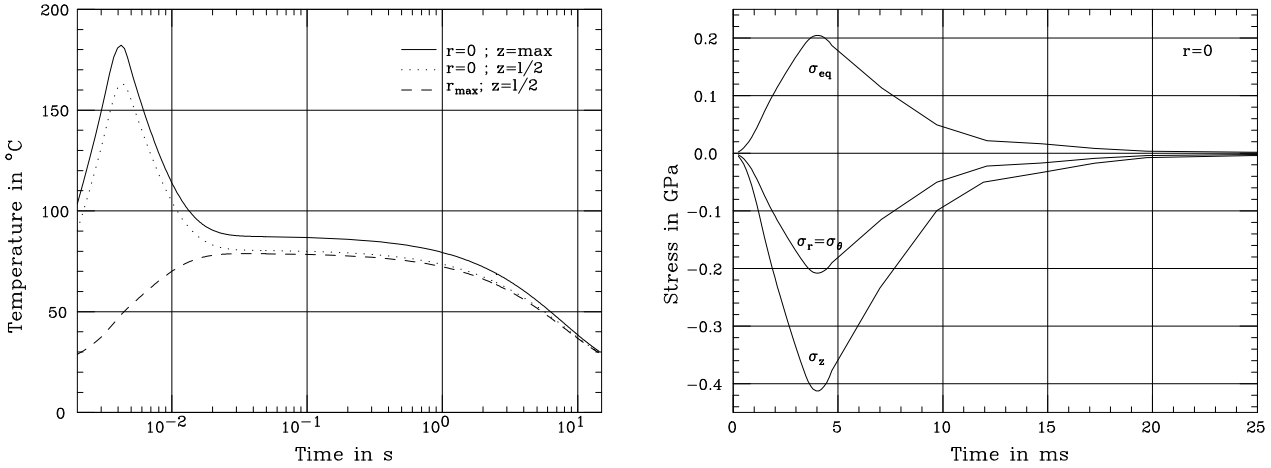

Figure 3: Time evolution of: a) temperature (left plot); b) stress components (right plot), induced by 6 ms beam pulse.

model). Finally, a file is written in the ANSYS system input format, containing the commands assigning an internal heat generation rate (energy per unit volume and time interval) to each node number.

The transient solution was obtained only for the first (most critical) rod, and for the first extraction with no repetition (20^{o}C initial temperature). The nominal 6 ms extracted beam was approximated by a trapezoidal pulse of 4.7 ms duration, normalised to $1.5{\cdot}10^{13}$ protons. Then, up to the end of the 14.4 s cycle, the heat generation was turned off and only heat conduction and cooling could take place, accompanied by release of the quasi-static thermal stress. Theoretical considerations as well as our calculations show that the dynamic effect of stress wave propagation is negligible in this case.

Table 1 summarises maximum temperature and stress, induced on axis of the first target rod. The ANSYS results compare quite well to the analytical one-dimensional solution with simplified assumptions [5]. The beryllium temperature rises up to 182^{o}C , dropping at the end of the cycle to 30^{o}C . Repeated cycles of 2 extractions ($1.5{\cdot}10^{13}$ protons each, separated by 2.76 s) lead to a maximum temperature of 245^{o}C (see Figure 4), safely below the melting point of 1280^{o}C . The time dependence of temperature and stress components (radial σ_r, longitudinal σ_z and von Mises equivalent σ_{eq}), at the point of maximum thermal load, is plotted in Figure 3. Both stress components are compressive on the beam axis, while at the radial surface of the rod the radial stress becomes zero, and the longitudinal stress becomes tensile. The maximum equivalent stress does not reach the elastic limit of beryllium (0.29 GPa) and just approaches the fatigue limit ($\pm$0.22 GPa), which augurs fair material life.

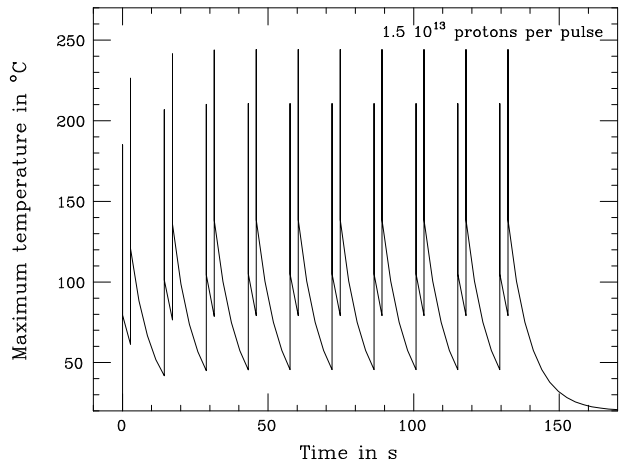

Figure 4: Thermal cycling of the first rod.

Table 1: Maximum temperatures and stresses induced by a single 6 ms beam pulse in the first rod.

		ANSYS	analytic
Temperature (^{o}C)	end of pulse	182	185
	end of cycle	30	29
Quasi-static stress (GPa)	radial (σ_r)	–0.21	–0.24
	longit.(σ_z)	–0.41	–0.47
	eqvl.(σ_{eq})	0.21	0.24

Acknowledgments

We are pleased to underline the contribution of A. Barisy, G. Del Torre, M. Gayoso, M. Goujon, A. Marchand, to the design and/or the achievement of this project.

3 REFERENCES

[1] 'Target Stations and Beam Dumps for the CERN SPS', by W. Kalbreier *et al.*, CERN SPS/ABT/77-3.

[2] 'CERN West Area Neutrino Facility Beam Alignment', by G. Catanesi *et al.*, to be published for this conference.

[3] 'FLUKA: Present Status and Future Developments', by A. Fassò *et al., IV Int. Conf. on Calorimetry in High Energy Physics*, La Biodola, Italy (Sept. 20–25 1993).

[4] 'ANSYS (Revision 5.1)', by Swanson Analysis Systems, *Inc.*, SASI/DN-P511:51, Houston, USA (Sept. 30 1994).

[5] 'Thermo-Mechanical Effects Induced by SPS Beam in a Beryllium Rod of the T9 Neutrino Target', by J.M. Zazula, M. Ross and S. Péraire, CERN SL/Note 95–90 (BT/TA).